JOURNAL OF VIROLOGY, Nov. 1996, p. 7811–7818
0022-538X/96/$04.00+0

Vol. 70, No. 11

A Mutation in the Puff Region of VP2 Attenuates the Myocarditic Phenotype of an Infectious cDNA of the Woodruff Variant of Coxsackievirus B3

KIRK U. KNOWLTON,[1]* EUN-SEOK JEON,[1] NEIL BERKLEY,[1] RAINER WESSELY,[1] AND SALLY HUBER[2]

Department of Medicine, University of California, San Diego, California 92103,[1] and Department of Pathology, University of Vermont, Burlington, Vermont 05405[2]

Received 2 May 1996/Accepted 25 July 1996

Coxsackievirus B3 (CVB3) infections induce myocarditis in humans and mice. Little is known about the molecular characteristics of CVB3 that activate the cellular immunity responsible for cardiac inflammation. Previous experiments have identified an antibody escape mutant (H310A1) of a myocarditic variant of CVB3 (H3) that attenuates the myocarditic potential of the virus in mice in spite of ongoing viral replication in the heart. We have cloned full-length infectious cDNA copies of the viral genome of both the wild-type myocarditic H3 variant of CVB3 and the antibody escape mutant H310A1. Progeny viruses maintained the myocarditic and attenuated myocarditic potential of the parent viruses, H3 and H310A1. The full sequence of the H3 viral cDNA is reported and compared with those of previously published CVB3 variants. Comparison of the full sequences of H3 and H310A1 viruses identified a single nonconserved mutation (A to G) in the P1 polyprotein region at nucleotide 1442 resulting in an asparagine-to-aspartate mutation in amino acid 165 of VP2. This mutation is in a region that corresponds to the puff region of VP2. Nucleotide 1442 of the H3 and H310A1 cDNA copies of the viral genome was mutated to change amino acid 165 of VP2 to aspartate and asparagine, respectively. The presence of asparagine at amino acid 165 of VP2 is associated with the myocarditic phenotype, while an aspartate at the same site reduces the myocarditic potential of the virus. In addition, high-level production of tumor necrosis factor alpha by infected BALB/c monocytes is associated with asparagine at amino acid 165 of VP2 as has been previously demonstrated for the H3 virus. These findings identify potentially important differences between the H3 variant of CVB3 and other previously published CVB3 variants. In addition, the data demonstrate that a point mutation in the puff region of VP2 can markedly alter the ability of CVB3 to induce myocarditis in mice and tumor necrosis factor alpha secretion from infected BALB/c monocytes.

Coxsackieviruses have been identified as important pathogens in myocarditis in children and adults; in addition, they may contribute to the pathogenesis of dilated cardiomyopathy. The precise mechanisms of tissue injury in myocarditis and cardiomyopathy are less clear. Certainly, coxsackieviruses induce cytopathology directly through infection and replication in myocardial cells (6, 20, 46). However, both clinical and experimental studies also implicate immunopathogenic mechanisms whereby activation of immune responses to either viral or cellular antigens results in myocardial damage and ventricular dysfunction (10). Most likely both forms of injury precipitate myocarditis and cardiomyopathy, with the relative contributions of virus- and immune-dependent mechanisms varying in different individuals or under different conditions.

A specific model of coxsackievirus B3 (CVB3; Nancy strain)-induced myocarditis was developed by Jack Woodruff and uses a highly myocarditic variant of CVB3 (CVB3w) that induces a severe acute inflammatory response in appropriate strains of infected mice. This CVB3 variant has been used by many investigators to study the immune response associated with myocarditis. Indeed, both Woodruff and Woodruff (45) and Huber and Lodge (14) demonstrated that BALB/c mice depleted of T lymphocytes developed minimal myocarditis despite high cardiac virus titers, indicating that in this strain of mice, myocarditis is primarily mediated through immune rather than viral mechanisms. Little is known about the viral determinants of coxsackieviruses that activate the T cells responsible for cardiac injury. It is therefore important to evaluate the molecular characteristics of distinct CVB3 variants which differ in their abilities to stimulate these pathogenic T cells. This approach has been valuable in understanding the pathogenesis of immunosuppression in mice infected with lymphocytic choriomeningitis virus (3).

A plaque-purified, highly myocarditic variant of CVB3w, H3, was previously isolated by one passage of CVB3w from the heart of an infected mouse (42). This plaque-purified variant is highly myocarditic in BALB/c mice (28, 42). A less myocarditic antibody escape mutant of H3 was previously isolated by incubating the H3 virus with a neutralizing monoclonal antibody, 10A1, and isolating the escape mutant H310A1 in HeLa cells (28, 42). Previously published data demonstrate that the H310A1 virus is able to infect the myocardium, but that the inflammatory response is severely attenuated compared with that of the H3 virus. Pathogenicity in H3 virus-infected mice correlates to the preferential induction of CVB3-immune $CD4^+$ T cells expressing the T_H1 cell phenotype, characterized by the production of high levels of gamma interferon (IFN-γ) and interleukin-2 (IL-2) but little or no IL-4 expression. CVB3-immune $CD4^+$ cells in H310A1 virus-infected mice express the T_H2 cell phenotype, producing high IL-4 and little IFN-γ or IL-2. The T_H2-rich $CD4^+$ cell population actively suppresses both immunopathogenic responses and myocarditis when adoptively transferred into H3 virus-infected animals (18, 19).

* Corresponding author. Mailing address: Department of Medicine, 8411, University of California, San Diego, 200 W. Arbor Dr., San Diego, CA 92103-8411. Phone: (619) 543-7346. Fax: (619) 543-7354. Electronic mail address: kknowlton@ucsd.edu.

The reasons for the difference in T_H subset responses induced by these variants is subject of active investigation. H310A1 virus usually replicates to significantly lower titers in vivo and in vitro than H3 virus and additionally stimulates meager cytokine responses (tumor necrosis factor alpha [TNF-α], IL-1, or IFN-α/β) in a macrophage/monocyte cell line (15) as well as in primary cultures of BALB/c splenic macrophages (13). Either reduction of viral antigen load or suppression of macrophage/monocyte activation may be pivotal in determining T_H subset differentiation during CVB3 infection (8).

Therefore, to begin to understand the mechanisms by which the Woodruff variant of CVB3 can induce the pronounced acute myocarditis and to identify regions of the virus that are important in activating the immune response, we report cloning of infectious cDNA copies of the genome of the H3 variant of CVB3 and the antibody escape mutant H310A1. The full sequence of the H3 variant is compared with the sequence of previously published infectious cDNAs of the Nancy variant of CVB3 (5, 22). We have also identified a single mutation in the puff region of VP2 in the H310A1 variant that confers an attenuated myocarditic potential to the myocarditic H3 variant of CVB3.

MATERIALS AND METHODS

Mice. BALB/c mice were originally obtained from Cumberland Farms (Clinton, Tenn.). Adult mice were derived from colonies of these mice maintained at the University of Vermont. MRL/++ male mice, 6 to 10 weeks of age, were kindly supplied by Ralph Budd, Department of Medicine, University of Vermont, from a breeding colony of these animals maintained at this institution.

Viruses. H3 and H310A1 viruses are previously described plaque-purified isolates of the Woodruff variant of CVB3 (42).

Isolation of viral RNA. After three cycles of freezing and thawing, virus from HeLa cells was treated with DNase I (Sigma) and RNase A (Sigma) (1 μg/ml) and then precipitated with 1 M NaCl and 10% polyethylene glycol 8000. The pellet was resuspended in SM buffer with proteinase K (Gibco/BRL) (0.1 mg/ml) and EDTA (0.02 M) and incubated for 15 min at 37°C. After 1% sodium dodecyl sulfate (Bio-Rad) was added, the RNA was incubated 30 min at 56°C. The RNA was then extracted with Tris-saturated phenol and chloroform-isoamyl alcohol, precipitated in isopropanol, and washed with 70% ethanol.

Generation of full-length cDNA copies of the viral genome. Sense and antisense primers were initially derived from published CVB3 sequences (22, 27, 39). Reverse transcriptase PCR (RT-PCR) was then performed by using Moloney murine leukemia virus H^- reverse transcriptase and 30 cycles of PCR (95°C for 5 min, then 55°C for 1 min, 72°C for 2 min, and 95°C for 1 min for 30 cycles, and finally 72°C for 7 min), using Exo^+ Deep Vent polymerase (New England Biolabs). Because of a significant number of sequence differences in the H3 virus compared with the sequence of the Nancy variant in the P2 and P3 regions of the virus (22, 27, 39), it was necessary to use low-stringency PCR (95°C for 5 min followed 95°C for 1 min; 50°C for 2 min and 72°C for 2 min for 40 cycles; then 72°C for 7 min). The PCR products were sequenced. Additional primers were then designed according to the new sequences. Each primer was approximately 30 nucleotides long, including unique 5′ *Not*I and a 3′ *Sal*I or *Cla*I restriction sites added for convenience in cloning. The PCR products were then cloned into pBluescript KS− (Stratagene). Eight fragments overlapping the entire viral genome were obtained. The full-length cDNA was constructed by ligating the overlapping fragments at convenient restriction sites into pBST KS− (Stratagene) or pBKCMV (Stratagene) (Fig. 1).

Transfection and isolation of recombinant virus. Large-scale plasmid preparations of the full-length cDNA were obtained by using Qiagen columns. Plasmid DNA was transfected into Cos cells by using a modified calcium phosphate precipitation protocol as previously described (23). Large-scale preparations of virus were obtained by transferring supernatant from transfected Cos cells to HeLa cell monolayers with a multiplicity of infection of less than 1.0.

Nucleotide sequencing. cDNA copies of the viral genome were sequenced by using dideoxy nucleotides and the T7 DNA polymerase Sequenase (United States Biochemical) as previously described (34). Full-length sequence for the H3 viral genome was confirmed by comparing the sequence derived from the H3 genome with the sequence of the H310A1 viral genome. Nucleic acid differences between H3 and H310A1 were confirmed by sequencing plasmid amplified from at least two separate viral preparations and from two to three separate bacterial colonies derived from ligation and transformation of the PCR products. The nucleic acid sequence of H3 virus at primer annealing sites was determined by sequencing separate PCR fragments of the viral genome amplified by using different primers.

Site-directed mutagenesis. Site-directed mutagenesis was performed by using the Sculpture reagents (Amersham). Oligonucleotides that anneal to nucleotides 1430 to 1451 for mutagenesis were designed as follows: VP2-N165D is 5′-GCA TCCGGATCCGACAAGTTGG, and VP2-D165N is 5′-GCATCCGGATCCA ACAAGTTGG. Mutations were generated in the 887-2089 cDNA fragment of the viral genome (Fig. 1). When confirmed by dideoxynucleotide sequencing, the mutated fragment was inserted into the full-length cDNA of the original H3 or H310A1 viral genome.

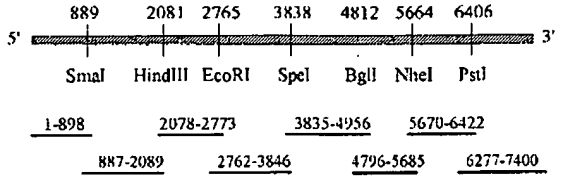

FIG. 1. Overlapping fragments of H3 virus used to clone full-length infectious cDNA. Restriction sites used for cloning of the H3 and H310A1 infectious cDNA copies of the viral genome are shown below the hatched bar representing the full-length cDNA. Their nucleic acid positions are noted above the hatched bar. Below the restriction sites are lines that represent the RT-PCR fragments that were used to generate the full-length cDNA, with the 5′ and 3′ ends noted above each fragment. The *Sma*I and *Eco*RI sites shown are not present in the original H3 sequence but are present in the infectious H3 cDNA because of primer design.

Organ virus titer. Hearts were removed aseptically, weighed, and homogenized in Dulbecco modified Eagle medium (DMEM) containing 2% fetal bovine serum (FBS). Cellular debris was removed by centrifugation at 300 × *g* for 10 min, and the titers of virus in the supernatants were determined by plaque-forming assay (42).

Isolation and sequencing viral RNA from infected hearts. Seven days after inoculation with the appropriate virus, RNA was isolated from the hearts of two mice infected with each variant of CVB3 (H3c, H310A1c, H3 VP2-N165D, and H310A1 VP2-D165N), for a total of eight separate RNA preparations. A fragment of the viral RNA, bp 887 to 2089, was amplified by RT-PCR, and the sequence of the virus at nucleic acid 1442 was determined by dideoxy nucleotide sequencing of at least two individual clones isolated from each PCR.

Infection of macrophage cells. A BALB/c-derived monocyte/macrophage line (J774A.1; American Type Culture Collection, Rockville, Md.) was maintained in DMEM–10% FBS. Approximately 10^5 cells per well were dispensed into 96-well tissue culture plates (Bellco) and exposed to 10^6 PFU of either H3 or H310A1 for 1 h at 37°C. The cells were washed, treated with a 1:100 dilution of horse anti-CVB3 (American Type Culture Collection) to eliminate extracellular virus, washed again, and cultured in 200 μl of DMEM–10% FBS for times ranging from 12 to 72 h. Supernatants of the triplicate cultures were removed for determination of TNF-α concentrations; the cells were retrieved by trypsinization (0.25% trypsin; GIBCO) and frozen and thawed three times, and the virus titer was determined by plaque-forming assay.

TNF-α assay. WEHI 164, subclone 13, cells (American Type Culture Collection) were grown in DMEM–10% FBS, centrifuged at 160 × *g*, washed, resuspended to 10^7 cells per ml, and incubated with 100 μCi of ^{51}Cr for 2 h at 37°C. The cells were washed four times and dispensed (2×10^4 cells per well) into 96-well tissue culture plates together with an equal volume of supernatant from the macrophage cultures. A standard curve for TNF-α-mediated cell lysis was established by using recombinant TNF-α (kindly supplied by Genentech, South San Francisco, Calif.) ranging in concentration from 1 to 1,000 U/ml. The plates were incubated at 37°C for approximately 15 h in a humidified 5% CO_2 incubator. Percent ^{51}Cr release and percent lysis of WEHI cells were measured.

Histology and image analysis. Hearts were fixed in 10% buffered formalin, sectioned, and stained with either hematoxylin and eosin (for inflammation) or Von Kossa stain (32) (for myocyte injury). Sections stained with Von Kossa stain were used for image analysis in transmitted light mode with an Olympus BX50 compound light microscope (4× objective lens; numerical aperture, 0.13). True-color digital images (640 by 480 pixels) were captured with a Sony DXC-960MD/LLP video camera connected via an RS170 cable to a video frame grabber on a Sun SPARCstation 5. Image processing, and analysis were accomplished with IMIX software (Princeton Gamma Tech, Inc., Princeton, N.J.). For determining the area of cardiac injury, the area of heart (square micrometers) in the total field was calculated on a binary image. The area of injury was determined on the color image by using the "true color" feature of the software. Final percent cardiac injury was calculated by dividing the area of injury by the total area of the heart.

Sections were graded blindly for cardiac inflammation by two of us, using a scale of 0 to 4 in which 0 represented no myocarditis, 1 represented 1 to 10 lesions, 2 represented 11 to 20 lesions, 3 represented 21 to 40 lesions, and 4 represented widespread and confluent inflammation.

Statistics. Statistical evaluations were performed by using either the Wilcoxon ranked score or the Student *t* test.

Nucleotide sequence accession number. The full nucleic acid sequence of the H3 variant of CVB3 is available through GenBank (accession number U57056).

5' Non-translated Region

3' Non-translated region

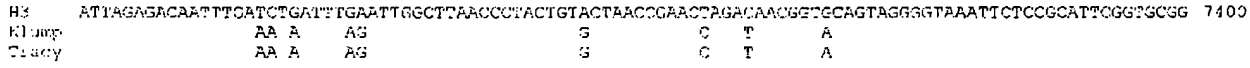

FIG. 2. Nucleic acid sequence comparison of untranslated regions of three fully sequenced infectious cDNA copies of the CVB3 genome. The cDNA-derived nucleic acid sequence for the H3 variant of CVB3 is shown in the top line, with different nucleic acids from the Nancy variant of CVB3 reported by Klump et al. (22) and Tracy et al. (39) shown below. A dash indicates no nucleotide reported at that site.

RESULTS

Cloning of infectious cDNA copies of H3 and H310A1. To obtain full-length infectious cDNA copies of H3 and H310A1 viral genomes, eight fragments were amplified by RT-PCR. Initial primer sequences were designed according to previously published CVB3 sequences (22, 27, 39). Because of the significant differences in the sequence of H3 compared with the previously published sequences for CVB3 in the P2 and P3 regions of the coxsackievirus, primers for amplification of the full P2-P3 region were designed at convenient restriction sites from partial H3 sequence of that region. These restriction sites were then used to reconstruct the full-length cDNA copies of the viral genome (Fig. 1). The full-length cDNA copies of the viral genome were inserted into the *Not*I-*Cla*I sites of pBluescript (Stratagene) or pBKCMV (Stratagene). Virus was obtained from the infectious cDNAs by transfection with a modified calcium phosphate precipitate as described in Materials and Methods. As negative controls, cells were mock transfected either without DNA or without calcium. Virus was not isolated from the mock-transfected cultured cells in either case. Virus derived from the infectious cDNA was neutralized with a CVB3-neutralizing monoclonal antibody (8A6) (16). Antibody neutralization and nucleotide sequencing confirmed that the virus was CVB3.

Nucleotide sequence of H3 cDNA. The full sequence of the H3 cDNA was obtained by using dideoxy sequencing techniques and compared with previously published CVB3 sequences. To exclude the possibility of PCR error in the sequence, the sequence was compared with the sequence of cDNA amplified from at least one other H3 viral preparation. The nucleic acid sequence of the untranslated region is shown in Fig. 2 and compared with previously published sequence of two infectious cDNA copies of CVB3 (22, 39). The amino acids that are distinct from those of previously published cDNA copies of CVB3 are shown in Table 1.

Compared with three previously published sequences of the Nancy strain of CVB3 (22, 27, 39), the H3 virus is 8.2% divergent (605 of 7,400 nucleotides) at the nucleic acid level. In each segment, 3.0% (22 of 742 nucleotides) in the 5′ untranslated region, 3.1% (92 of 3,003 nucleotides) in the P1 region, 8.1% (162 of 1,992 nucleotides) in the P2 region, 16.0% (320 of 2,004 nucleotides) in the P3 region, and 9.0% (9 of 100 nucleotides) in the 3′ untranslated region of H3 are divergent from the three other published sequences of CVB3. Compared with deduced amino acid sequences of fully sequenced infectious cDNAs of the Nancy strain of CVB3 (22, 39), 22 of 2,185 (1.0%) amino acids (aa) of the H3 virus are divergent. Of these, 9 of 1,001 (0.9%), 9 of 428 (2.1%), and 15 of 756 (2.0%) amino acid differences are in P1, P2, and P3 regions, respectively (Table 1). There is also a serine at aa 151 of VP2 of H3, the same as in the CVB3 RD isolate, which allows infection of CVB3 in RD cells by using the complement-binding protein decay-accelerating factor (CD55) as a receptor (2, 26).

A single mutation in the puff region of VP2 is responsible for the H310A1 myocarditic phenotype. Nucleotide sequencing of the full lengths of both H3 and H310A1 cDNA copies of the viral genome identified a single mutation in H310A1 compared with the H3 virus. There is a change in nucleic acid 1442 from

TABLE 1. Amino acid differences among three myocarditic infectious CVB3 cDNAs that have been fully sequenced[a]

Protein region	aa	H3 (10A1)[b]	Klump[c]	Tracy[d]
VP4	16	**G**	R	R
	51	**S**	G	G
VP2	13	**V**	A	V
	108	**I**	V	V
	138	**N**	D	D
	151	**S**	**T**[e]	S
	165	**N (D)**	N	N
	245	**I**	V	V
VP3	155	**V**	I	V
	178	**Y**	F	F
VP1	45	**S**	G	G
	80	**E**	K	K
	180	**V**	I	I
	264	**Q**	Q	**R**
2A	32/35[f]	**N**	S	S
	44/47	**A**	A	**T**
	54/57	**R**	Q	Q
	78/81	**I**	L	L
2B	13	**F**	F	**L**
2C	3	**G**	S	S
	23	**I**	V	V
2C	96	**S**	A	A
	181	**K**	N	N
	271	**E**	D	D
	322	**A**	T	T
3A	21	**R**	A	A
	48	**V**	I	I
	68	**I**	L	L
3B	6	**I**	V	V
	12	**K**	R	R
3C	17	**T**	T	**R**
3D	11	**E**	D	D
	37	**D**	N	N
	45	**V**	A	A
	52	**V**	A	A
	75	**M**	L	L
	136	**R**	K	K
	165	**A**	I	I
	259	**S**	T	T
	350	**D**	G	G
	372	**V**	A	V
	454	**I**	L	L

[a] Amino acids not found in the other two sequences are indicated in boldface. The sequence of an infectious nonmyocarditic CVB3 cDNA (5) has also been reported.

[b] Data for H3 and, in parentheses, H310A1 (at aa 165 of VP2) are from this report.

[c] From reference 22.

[d] Data from reference 39.

[e] Amino acid 152 of VP2 is a serine in the RD virus phenotype reported by Lindberg et al. (26).

[f] Because of two potential proteolytic sites at the beginning of protease 2A, numbers from both sites are shown.

an A to G that results in a change in aa 165 of VP2 from an asparagine to aspartate in H310A1. This mutation in H310A1 was confirmed by sequencing plasmids from three separate bacterial colonies derived from ligation and transformation of the PCR products and RT-PCR amplification of a separate isolation of H310A1 viral RNA. Alignment of CVB3 with human rhinovirus 14 (HRV14) and poliovirus shows that this mutation occurs in a region that corresponds to the puff regions of HRV14 and poliovirus (25).

Myocarditic potential of CVB3 is decreased with aspartate at aa 165 of VP2. Mice were infected with virus derived from the infectious cDNA copies of the viral genome. The H3-cDNA derived virus (H3c) maintained its ability to induce myocarditis in BALB/c mice (*H-2d*) but not in MRL/++ mice (*H-2k*). H3 viral pathogenicity was measured both by induction of cardiac inflammation as observed in high-magnification views of hematoxylin-and-eosin-stained heart sections (Fig. 3) and by induction of myocyte injury as detected by Von Kossa staining (Table 2; Fig. 4). Distribution of damaged areas which stain black-brown with Von Kossa stain (32) is readily discernible in low-magnification views of heart cross sections in Fig. 4. H310A1 cDNA-derived virus (H310A1c) induced minimal cardiac inflammatory response in infected mice, but both the number and size of inflammatory lesions were substantially less than observed in animals infected with the pathogenic (H3c) virus, even though H310A1c infected the heart (Table 2; Fig. 3). Minimal or no myocyte injury was observed with this virus variant (Table 2; Fig. 4). H3c-H310A1c chimeric viruses were made by exchanging the *Sma*I (889)-*Hin*dIII (2081) fragments. Since the myocarditic potential of the chimeric viruses corresponded with that of the original *Sma*I-*Hin*dIII fragment, point mutations were made at nucleotide 1442. H3 VP2-N165D was generated by mutating nucleotide 1442 from A to G in the H3 cDNA, thus changing the amino acid sequence from asparagine to aspartate. Similarly, H310A1 VP2-D165N was generated by changing nucleotide 1442 from G to A in the H310A1 cDNA. Mice infected with the virus derived from the H3 VP2-N165D cDNA had significantly less myocarditis and cell damage than mice infected with virus derived from the H310A1 VP2-D165N cDNA (Table 2; Fig. 3). Virus isolated from the hearts of mice infected with H3c, H310A1c, H3 VP2-N165D, and H310A1 VP2-D165N viruses maintain the nucleic acid sequence of the parent viral cDNA at the codon for aa 165 of VP2. These findings confirm that an asparagine-to-aspartate mutation at aa 165 significantly attenuates the ability of CVB3 to induce myocarditis in BALB/c mice.

Previous experiments have shown that the H3 virus can infect BALB/c monocytes and induce release of numerous cytokines, including TNF-α, IL-1, and IFN-α/β, from the cells. It has been previously shown that the H310A1 virus is not able to infect the cells as efficiently or induce as potent as cytokine response (15). To determine whether the single amino acid change between H3 and H310A1 viruses alters macrophage-associated cytokine responses, TNF-α production was measured in BALB/c monocytes infected with the H3c, H310A1c, H3 VP2-N165D, and H310A1 VP2-D165N recombinant viruses. Elevated TNF-α production correlated to infections with the virus variants having an asparagine at aa 165 of VP2 (Fig. 5). Other macrophage-associated cytokines were not evaluated in this study.

DISCUSSION

It has been clearly shown that CVB3 infection in mice activates an acute immune response which peaks at about 7 days after infection (7, 21, 42, 43, 45). This acute immune response in the heart has been extensively studied by using the Woodruff variant of CVB3 (44, 45). In addition to the myocarditic response of CVB3 infection, some forms of CVB3 have been shown to induce hepatic necrosis as well as myocarditis in BALB/c mice (9). The H3 variant of CVB3 was selected because of its relative cardiotrophic/myocarditic potential in BALB/c mice. High levels of virus are obtained from the hearts of mice that have been infected with this variant of CVB3 (12). In contrast, less myocarditic CVB3 variants (CVB3o and H310A1) replicate in the heart to high titers, yet the amount of cardiac inflammation is very modest, with both fewer numbers of mononuclear cells per lesion and fewer lesions per heart

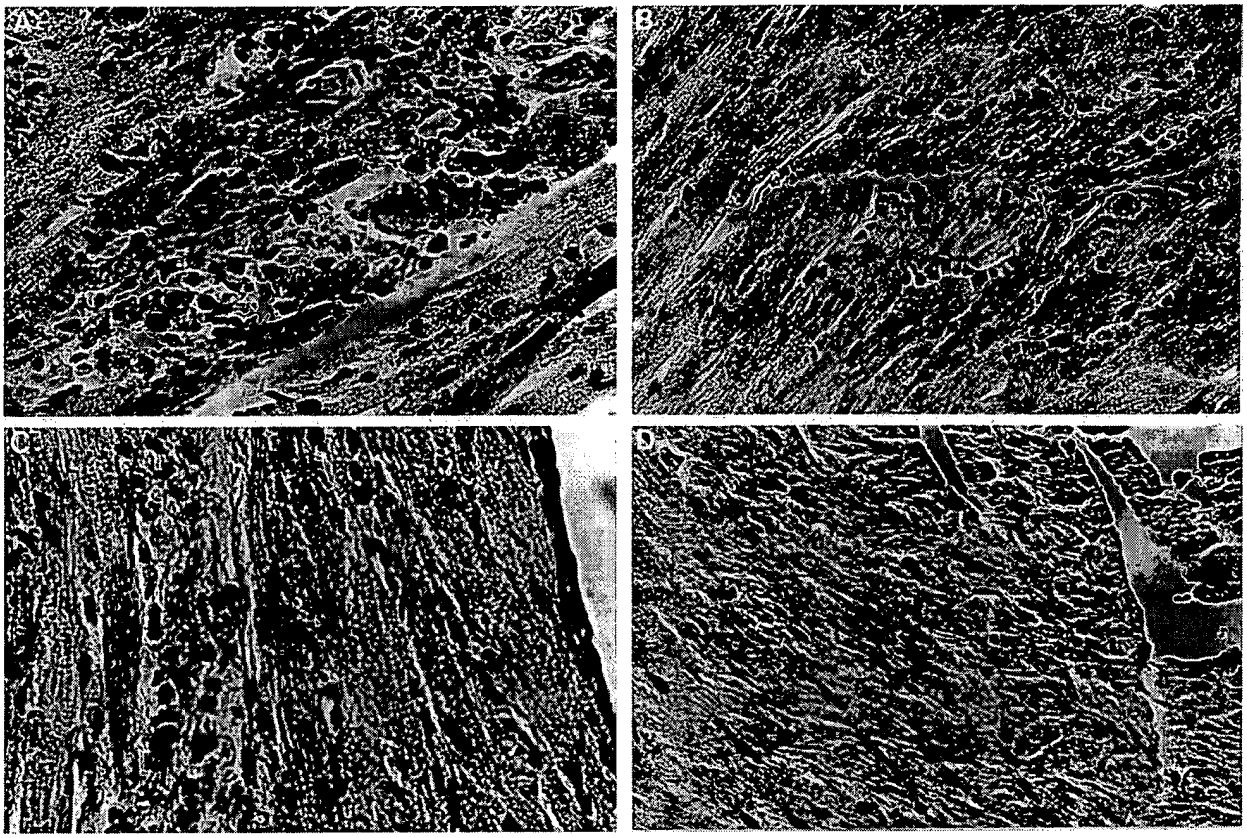

FIG. 3. Hematoxylin-and-eosin staining of hearts from mice infected with cDNA-derived viruses. Mice were inoculated by intraperitoneal injection with 10^4 PFU of cDNA-derived viruses in 0.5 ml of phosphate-buffered saline and harvested after 7 days. (A and C) The typical myocarditis seen when mice are infected with virus that contains an asparagine at aa 165 of VP2 as in H3c (A) and H310A1 VP2-D165N (C). (B and D) Lack of inflammation in hearts from animals infected with virus which has an aspartate at aa 165 of VP2 as in H310A1 (B) and H3 VP2-N165D (D). Imaged at ×200 magnification.

section than observed in H3 virus-infected hearts. Additionally, there is a qualitative difference in the type of infiltrating mononuclear cells, with fewer T cells in H310A1-infected hearts than in H3 virus-infected hearts (13, 17). The H3 variant of the Woodruff virus induces both pathogenic $CD4^+$ T cells to viral epitopes and $CD8^+$ T cells to myocardial antigens (14, 16, 19). Precursor frequency analyses of the splenic $CD4^+$ T cells correlate the induction of myocarditis to T_H1 cell responses. Similarly, myocarditic mice have high levels of IL-2 and low levels of IL-4 circulating in their sera, while disease-resistant mice have the opposite pattern (low IL-2 and high IL-4) (18). The preferential activation of T_H2 cells in H310A1 virus-infected animals most likely suppresses the autoimmune $CD8^+$ T-cell response which is primarily pathogenic in myocarditic mice (19, 28). Administration of an exogenous cytokine (IFNγ, IFNβ, or IL-2) to H310A1-infected mice has been shown to produce substantial myocarditis (19). These results imply that H310A1 virus cannot activate the immune response because of an inability to stimulate cytokines. The identification of a precise mutation in the H310A1 virus that mediates this unique viral phenotype will facilitate an understanding of how distinct viruses can activate different immunologic responses. Such characteristics may have important implications in the myocarditic potential of CVB3 infection in humans as well.

Previous studies on poliovirus have suggested that changes in the 5′ untranslated region and the capsid region can have an

TABLE 2. Myocarditis score, myocardial injury by Von Kossa stain (32), and heart virus titer in BALB/c mice infected with each of the cDNA derived viruses[a]

Virus	Myocarditis score (avg ± SE)	% of myocardium stained with Von Kossa stain (avg ± SE)	Heart virus titer (log PFU/100 mg of tissue); avg ± SE)
H3c	2.08 ± 1.00	17.3 ± 4.5	5.32 ± 0.13
H310A1c	0.33 ± 0.49[b]	1.8 ± 0.6[b]	4.92 ± 0.13[b]
H3 VP2-N165D	0.75 ± 0.62[b]	2.8 ± 1.1[b]	4.77 ± 0.14[b]
H310A1 VP2-D165N	1.83 ± 0.58	14.7 ± 3.0	5.51 ± 0.14

[a] There were six mice in each group. Scoring was done as described in Materials and Methods.
[b] $P < 0.05$ compared with H3.

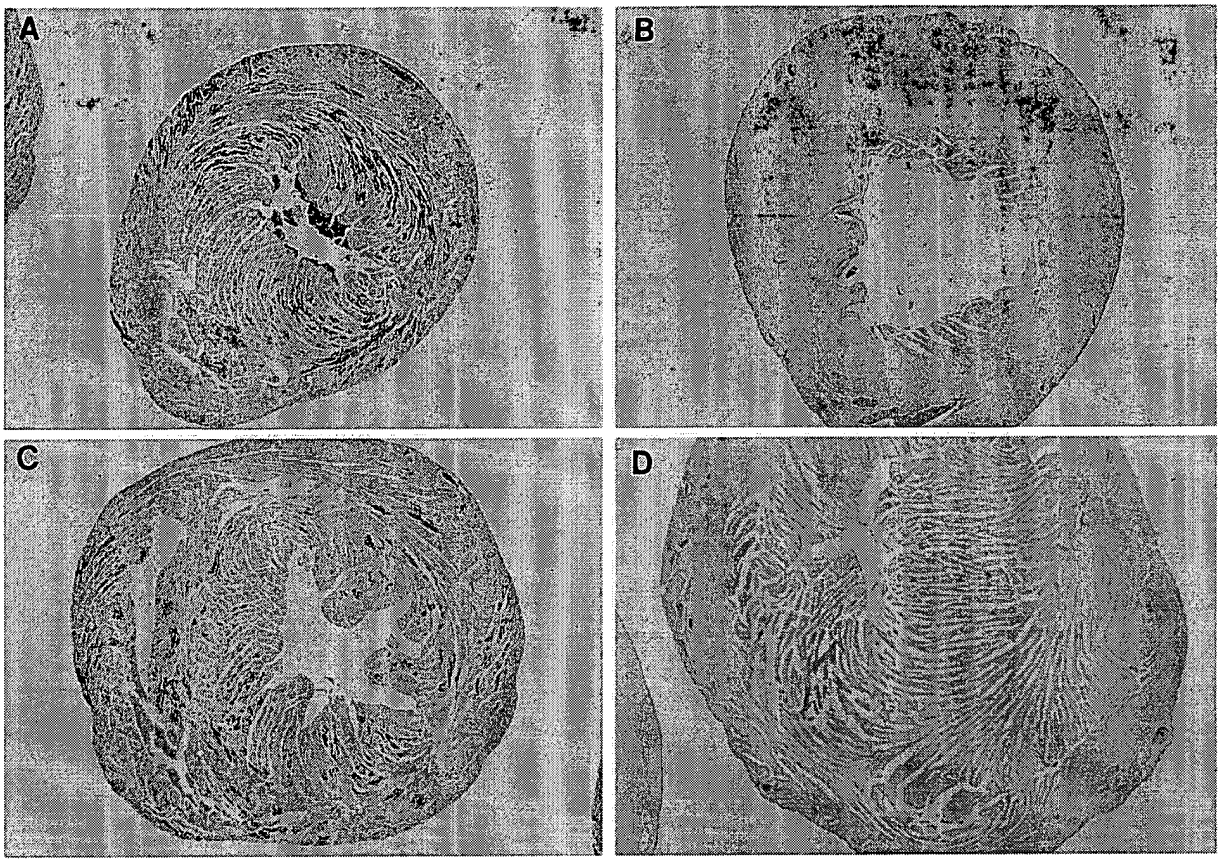

FIG. 4. Von Kossa staining of hearts from mice infected with cDNA-derived viruses showing cardiac injury. Sections from hearts depicted in Fig. 3 were stained with Von Kossa stain. (A) H3c virus-infected heart; (B) H310A1c virus-infected heart; (C) H3 VP2-N165D-infected heart; and (D) H310A1 VP2-D165N-infected heart. Necrotic areas stain black-brown. Imaged at ×10 magnification.

effect on poliovirus neurovirulence (1, 29, 31, 41). Similarly, it has been shown that in CVB4, a single mutation in an external loop of VP1 confers virulence in a pancreatitis model (4). CVB3 virulence can be attenuated by a mutation in an external loop of VP1 (47, 48). The 5′ untranslated region of CVB3 has also been shown to play an important role in CVB3-induced viral heart disease (40). A mutation at nucleic acid 234 in the 5′ untranslated region of the genome alters the ability of the virus to induce myocarditis even though the virus can still replicate in the murine heart. The previously reported mutations are clearly distinct from that which is documented in this report. These findings suggest that multiple mechanisms may be important in the stimulation of an immune response and generation of a myocarditic phenotype.

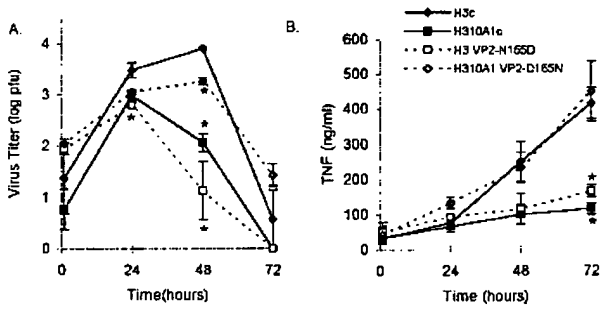

FIG. 5. Induction of TNF-α in BALB/c monocytes in culture. The J774A.1 monocyte/macrophage cell line was infected with the H3, H310A1, H3 VP2-N165D, and H310A1 VP2-D165N viral variants at a multiplicity of infection of 10:1. (A) Amounts of virus retrieved from the cells at various time points. Time zero is obtained after 1 h of incubation with the virus. (B) Concentrations of TNF-α in the extracellular media of infected cells. The data represent the means ± standard errors of three samples. *, $P < 0.05$ compared with H3 virus.

Sequencing of antibody escape mutants of poliovirus and rhinovirus have identified potential binding sites for viral neutralizing antibodies (30, 33, 38). In poliovirus, the immunodominant epitope II as defined by Minor et al. (30) is formed by residues from the internal insertion in VP2 (aa 127 to 185) and the internal insertions in VP1 (aa 207 to 237) and the carboxy terminus of VP2 (11). The crystal structure of HRV14 and alignment of HRV14 with poliovirus identify a similar antigenic epitope in HRV14 known as NIm II, made up of the internal insertion in VP2 (aa 128 to 169) and part of VP1 (aa 210) (33). These antigenic neutralization sites are in a hypervariable region also known as the puff region, which is located predominantly on the exterior of the virus capsid and is one of the protein regions in poliovirus which line the rim of the canyon floor (11). This region is referred to as the immunodominant region in rhinovirus (25, 33), but it is not known if the puff region in CVB is immunodominant. Figure 6 compares the amino acid sequence of the puff region of VP2 with

```
CVB3 H3       128  PEAEMGCATL NNT.PSSAFJ LGGDSAKEFA DKPVASGSNK LVQRVVYNAG MGVGVGNLTI FPH  189
CVB3 H310A1                                                    D
CVB3 Tracy                 D
CVB3 Klump                 D              T
CVB3 RD                    D

HRV14         128  PEHQLASHEG GNVSVKYTFT HPGERGIDLS SA...NEVGG PVKDVIYNM. NGTLLGNLLI FPH  186
```

FIG. 6. Protein alignment of the puff regions of VP2 in distinct CVB3 variants and in HRV14. Approximate protein alignment (25) of the puff region of VP2 is shown for five CVB3 variants, H3, H310A1, Tracy (39), Klump (22), and CVB3 RD (26), and for HRV14 (37). Amino acids for CVB3 variants that are different from those for the H3 virus are shown in boldface below the H3 sequence. A threonine-to-serine mutation at aa 138 in CVB3 RD allows the virus to infect RD cells (26). The locations of previously documented antibody escape mutants in HRV14 (33, 35, 36) are shown as boldface and underlined in the HRV14 sequence.

known mutations in CVB3 variants. Some of these changes are known to affect receptor binding or the potential of the virus to induce myocarditis. Sequences of previously documented antibody escape mutants in immunodominant loop II of VP2 in HRV14 are shown for comparison.

Lindberg et al. (26) identified a threonine-to-serine mutation at aa 151 of VP2 in this same puff region of CVB3 that alters receptor binding of CVB3 to the complement-binding protein decay-accelerating factor (CD55) (2, 26). Since this prominent loop lines the rim of the capsid's canyon floor in poliovirus, it may be an important component of the virus-receptor interaction, and mutations in this region may alter accessibility of the receptor to its binding site. Both the myocarditic Tracy cDNA (39)- and H3 cDNA-derived viruses have a serine at aa 151 of VP2. Since the 10A1 antibody was originally derived as an antibody that bound to cultured neonatal mouse cells and inhibited CVB3 infection (43), it is possible that the mutation that we have observed in the puff region of VP2 can also alter virus-receptor interactions. However, preliminary data show that both the H3 and H310A1 viruses can infect isolated adult BALB/c myocytes, as determined by immunocytofluorescence with an anti-CVB3 antibody (24). Alternatively, some of the neutralizing effects of the 10A1 antibody may be secondary to direct binding of the antibody to the virus, thus preventing interaction of the virus with its receptor. It is also possible that this antibody escape mutant has an altered myocarditic phenotype secondary to alterations in the manner in which this antigenic region stimulates the cellular and/or humoral immune response.

ACKNOWLEDGMENTS

We thank Douglas Taatjes and Anthony Quinn for expert help in performing the image analysis.

This work was supported by NIH grants HL-02618 to K.U.K., American Heart Association grant AHA CA-94-276 to K.U.K., a Korean Science and Engineering Foundation postdoctoral fellowship to E.-S.J., and Deutsche Forschunsgemeinschaft grant We 1811/1-1 to R.W.

REFERENCES

1. **Almond, J. W.** 1987. The attenuation of poliovirus neurovirulence. Annu. Rev. Microbiol. **41**:153–180.
2. **Bergelson, J. M., J. G. Mohanty, R. L. Crowell, N. F. St. John, D. M. Lublin, and R. W. Finberg.** 1995. Coxsackievirus B3 adapted to growth in RD cells binds to decay-accelerating factor (CD55). J. Virol. **69**:1903–1906.
3. **Borrow, P., C. F. Evans, and M. B. Oldstone.** 1995. Virus-induced immunosuppression: immune system-mediated destruction of virus-infected dendritic cells results in generalized immune suppression. J. Virol. **69**:1059–1070.
4. **Caggana, M., P. Chan, and A. Ramsingh.** 1993. Identification of a single amino acid residue in the capsid protein VP1 of coxsackievirus B4 that determines the virulent phenotype. J. Virol. **67**:4797–4803.
5. **Chapman, N. M., Z. Tu, S. Tracy, and C. J. Gauntt.** 1994. An infectious cDNA copy of the genome of a non-cardiovirulent coxsackievirus B3 strain: its complete sequence analysis and comparison to the genomes of cardiovirulent coxsackieviruses. Arch. Virol. **135**:115–130.
6. **Chow, L. H., K. W. Beisel, and B. M. McManus.** 1992. Enteroviral infection of mice with severe combined immunodeficiency. Evidence for direct viral pathogenesis of myocardial injury. Lab. Invest. **66**:24–31.
7. **Chow, L. H., C. J. Gauntt, and B. M. McManus.** 1991. Differential effects of myocarditic variants of coxsackievirus B3 in inbred mice. A pathologic characterization of heart tissue damage. Lab. Invest. **64**:55–64.
8. **Fitch, F. W., M. D. McKisic, D. W. Lancki, and T. F. Gajewski.** 1993. Differential regulation of murine T lymphocyte subsets. Annu. Rev. Immunol. **11**:29–48.
9. **Grun, J. B., M. Schultz, S. D. Finkelstein, R. L. Crowell, and B. J. Landau.** 1988. Pathogenesis of acute myocardial necrosis in inbred mice infected with coxsackievirus B3. Microb. Pathog. **4**:417–430.
10. **Hamrell, B. B., S. A. Huber, and K. O. Leslie.** 1994. Reduced unloaded sarcomere shortening velocity and a shift to a slower myosin isoform in acute murine coxsackievirus myocarditis. Circ. Res. **75**:462–472.
11. **Hogle, J. M., M. Chow, and D. J. Filman.** 1985. Three-dimensional structure of poliovirus at 2.9 Å resolution. Science **229**:1358–1365.
12. **Huber, S. A., C. Haisch, and P. A. Lodge.** 1990. Functional diversity in vascular endothelial cells: role in coxsackievirus tropism. J. Virol. **64**:4516–4522.
13. **Huber, S. A.** Unpublished data.
14. **Huber, S. A., and P. A. Lodge.** 1984. Coxsackievirus B-3 myocarditis in Balb/c mice. Evidence for autoimmunity to myocyte antigens. Am. J. Pathol. **116**: 21–29.
15. **Huber, S. A., A. Moraska, and M. Choate.** 1992. T cells expressing the γδ T-cell receptor potentiate coxsackievirus B3-induced myocarditis. J. Virol. **66**:6541–6546.
16. **Huber, S. A., A. Moraska, and M. Cunningham.** 1994. Alterations in major histocompatibility complex association of myocarditis induced by coxsackievirus B3 mutants selected with monoclonal antibodies to group A streptococci. Proc. Natl. Acad. Sci. USA **91**:5543–5547.
17. **Huber, S. A., A. Mortensen, and G. Moulton.** 1996. Modulation of cytokine expression by $CD4^+$ T cells during coxsackievirus B3 infections of BALB/c mice initiated by cells expressing the $\gamma\delta^+$ T-cell receptor. J. Virol. **70**:3039–3044.
18. **Huber, S. A., and B. Pfaeffle.** 1994. Differential Th1 and Th2 cell responses in male and female BALB/c mice infected with coxsackievirus group B type 3. J. Virol. **68**:5126–5132.
19. **Huber, S. A., J. Polgar, P. Schultheiss, and P. Schwimmbeck.** 1994. Augmentation of pathogenesis of coxsackievirus B3 infections in mice by exogenous administration of interleukin-1 and interleukin-2. J. Virol. **68**:195–206.
20. **Kandolf, R., A. Canu, and P. H. Hofschneider.** 1985. Coxsackie B3 virus can replicate in cultured human foetal heart cells and is inhibited by interferon. J. Mol. Cell Cardiol. **17**:167–181.
21. **Kandolf, R., K. Klingel, H. Mertsching, A. Canu, C. Hohenadl, R. Zell, B. Y. Reimann, A. Heim, B. M. McManus, and A. K. Foulis.** 1991. Molecular studies on enteroviral heart disease: patterns of acute and persistent infections. Eur. Heart J. **12**(Suppl. D):49–55.
22. **Klump, W. M., I. Bergmann, B. C. Muller, D. Ameis, and R. Kandolf.** 1990. Complete nucleotide sequence of infectious coxsackievirus B3 cDNA: two initial 5′ uridine residues are regained during plus-strand RNA synthesis. J. Virol. **64**:1573–1583.
23. **Knowlton, K. U., E. Baracchini, R. S. Ross, A. N. Harris, S. A. Henderson, S. M. Evans, C. C. Glembotski, and K. R. Chien.** 1991. Co-regulation of the atrial natriuretic factor and cardiac myosin light chain-2 genes during alpha-adrenergic stimulation of neonatal rat ventricular cells. Identification of cis sequences within an embryonic and a constitutive contractile protein gene which mediate inducible expression. J. Biol. Chem. **266**:7759–7768.
24. **Knowlton, K. U., and E.-S. Jeon.** Unpublished data.
25. **Liljas, L., A. M. Lindberg, and U. Pettersson.** 1993. Modelling of the tertiary structure of coxsackievirus B3 from the structure of poliovirus and rhinovirus. Scand. J. Infect. Dis. Suppl. **88**:15–24.
26. **Lindberg, A. M., R. L. Crowell, R. Zell, R. Kandolf, and U. Pettersson.** 1992. Mapping of the RD phenotype of the Nancy strain of coxsackievirus B3. Virus Res. **24**:187–196.
27. **Lindberg, A. M., P. O. Stalhandske, and U. Pettersson.** 1987. Genome of coxsackievirus B3. Virology **156**:50–63.
28. **Loudon, R. P., A. F. Moraska, S. A. Huber, P. Schwimmbeck, and P. Schultheiss.** 1991. An attenuated variant of coxsackievirus B3 preferentially induces immunoregulatory T cells in vivo. J. Virol. **65**:5813–5819.

29. **Macadam, A. J., D. M. Stone, J. W. Almond, and P. D. Minor.** 1994. The 5′ noncoding region and virulence of poliovirus vaccine strains. Trends Microbiol. **2**:449–454.
30. **Minor, P. D., M. Ferguson, D. M. Evans, J. W. Almond, and J. P. Icenogle.** 1986. Antigenic structure of polioviruses of serotypes 1, 2, and 3. J. Gen. Virol. **67**:1283–1291.
31. **Murray, M. G., J. Bradley, X. F. Yang, E. Wimmer, E. G. Moss, and V. R. Racaniello.** 1988. Poliovirus host range is determined by a short amino acid sequence in neutralization antigenic site I. Science **241**:213–215.
32. **Pearse, A. G. E.** 1972. Histochemistry: theoretical and applied, p. 1138–1139. Williams & Wilkins, Baltimore.
33. **Rossmann, M. G., E. Arnold, J. W. Erickson, E. A. Frankenberger, J. P. Griffith, H. J. Hecht, J. E. Johnson, G. Kamer, M. Luo, and A. G. Mosser.** 1985. Structure of a human common cold virus and functional relationship to other picornaviruses. Nature (London) **317**:145–153.
34. **Sambrook, J., E. F. Fritsch, and T. Maniatis.** 1989. Molecular cloning: a laboratory manual, 2nd ed. Cold Spring Harbor Laboratory, Cold Spring Harbor, N.Y.
35. **Sherry, B., A. G. Mosser, R. J. Colonno, and R. R. Rueckert.** 1986. Use of monoclonal antibodies to identify four neutralization immunogens on a common cold picornavirus, human rhinovirus 14. J. Virol. **57**:246–257.
36. **Sherry, B., and R. Rueckert.** 1985. Evidence for at least two dominant neutralization antigens on human rhinovirus 14. J. Virol. **53**:137–143.
37. **Stanway, G., P. J. Hughes, R. C. Mountford, P. D. Minor, and J. W. Almond.** 1984. The complete nucleotide sequence of a common cold virus: human rhinovirus 14. Nucleic Acids Res. **12**:7859–7875.
38. **Tormo, J., D. Blaas, N. R. Parry, D. Rowlands, D. Stuart, and I. Fita.** 1994. Crystal structure of a human rhinovirus neutralizing antibody complexed with a peptide derived from viral capsid protein VP2. EMBO J. **13**:2247–2256.
39. **Tracy, S., N. M. Chapman, and Z. Tu.** 1992. Coxsackievirus B3 from an infectious cDNA copy of the genome is cardiovirulent in mice. Arch. Virol. **122**:399–409.
40. **Tu, Z., N. M. Chapman, G. Hufnagel, S. Tracy, J. R. Romero, W. H. Barry, L. Zhao, K. Currey, and B. Shapiro.** 1995. The cardiovirulent phenotype of coxsackievirus B3 is determined at a single site in the genomic 5′ nontranslated region. J. Virol. **69**:4607–4618.
41. **Ubertini, T. R., C. Cioni, L. Perini, and S. Gagnoni.** 1988. Non-neurovirulent, genetically stable clone of poliovirus (Sabin type III vaccine strain). Vaccine **6**:481–482.
42. **Van Houten, N., P. E. Bouchard, A. Moraska, and S. A. Huber.** 1991. Selection of an attenuated coxsackievirus B3 variant, using a monoclonal antibody reactive to myocyte antigen. J. Virol. **65**:1286–1290.
43. **Weller, A. H., K. Simpson, M. Herzum, N. Van Houten, and S. A. Huber.** 1989. Coxsackievirus-B3-induced myocarditis: virus receptor antibodies modulate myocarditis. J. Immunol. **143**:1843–1850.
44. **Woodruff, J. F.** 1980. Viral myocarditis. A review. Am. J. Pathol. **101**:425–484.
45. **Woodruff, J. F., and J. J. Woodruff.** 1974. Involvement of T lymphocytes in the pathogenesis of coxsackie virus B3 heart disease. J. Immunol. **113**:1726–1734.
46. **Yoneda, S., K. Senda, and K. Hayashi.** 1979. Experimental study of virus myocarditis in culture. Jpn. Circ. J. **43**:1048–1054.
47. **Zhang, H., N. W. Blake, X. OuYang, Y. A. Pandolfino, P. Morgan-Capner, and L. C. Archard.** 1995. A single amino acid substitution in the capsid protein VP1 of coxsackievirus B3 (CVB3) alters plaque phenotype in Vero cells but not cardiovirulence in a mouse model. Arch. Virol. **140**:959–966.
48. **Zhang, H. Y., G. E. Yousef, L. Cunningham, N. W. Blake, X. OuYang, T. A. Bayston, R. Kandolf, and L. C. Archard.** 1993. Attenuation of a reactivated cardiovirulent coxsackievirus B3: the 5′-nontranslated region does not contain major attenuation determinants. J. Med. Virol. **41**:129–137.